

See discussions, stats, and author profiles for this publication at: <https://www.researchgate.net/publication/231680533>

# Multisite Recognition of Aqueous Dipeptides by Oligoglycine Arrays Mixed with Guanidinium and Other Receptor Units at the Air–Water Interface

ARTICLE *in* LANGMUIR · MAY 1999

Impact Factor: 4.46 · DOI: 10.1021/la981047p

CITATIONS

54

READS

6

## 4 AUTHORS, INCLUDING:



**Katsuhiko Ariga**

National Institute for Materials Science

622 PUBLICATIONS 21,075 CITATIONS

SEE PROFILE



**Xiao Zha**

Sichuan Tumor Hospital and Institute

41 PUBLICATIONS 662 CITATIONS

SEE PROFILE



**Toyoki Kunitake**

FAIS

670 PUBLICATIONS 20,404 CITATIONS

SEE PROFILE

# Multisite Recognition of Aqueous Dipeptides by Oligoglycine Arrays Mixed with Guanidinium and Other Receptor Units at the Air–Water Interface

Katsuhiko Ariga,<sup>†</sup> Ayumi Kamino, Xiao Cha,<sup>‡</sup> and Toyoki Kunitake<sup>\*,§</sup>

Supermolecules Project, JST (formerly JRDC), Kurume Research Park, 2432 Aikawa, Kurume 839-0861, Japan

Received August 18, 1998. In Final Form: March 11, 1999

Equimolar mixed monolayers of dioctadecyl glycyglycinamide amphiphile ( $2C_{18}BGly_2NH_2$ ) with other functional amphiphiles bearing guanidinium, pyridine, and alcoholic OH groups were prepared on water, and the binding of aqueous dipeptides to these monolayers was investigated by  $\pi$ -A isotherm measurement, FT-IR spectroscopy, and XPS elemental analysis. The binding behavior of GlyLeu to the mixed monolayer of  $2C_{18}BGly_2NH_2$  and guanidinium amphiphile ( $2C_{18}BGua$ ) was analyzed by a Langmuir isotherm to give a saturation guest/amphiphile ratio ( $\alpha$ ) of 0.46 and a binding constant ( $K$ ) of  $6400\text{ M}^{-1}$ . The former value indicates that the binding site for one GlyLeu molecule was formed cooperatively by the two monolayer components. The binding constant is much enhanced relative to those observed for the  $2C_{18}BGly_2NH_2$  single-component monolayer ( $35\text{ M}^{-1}$ ) and an equimolar mixed monolayer of  $2C_{18}BGly_2NH_2$  and benzoic acid amphiphile ( $2C_{18}BCOOH$ ) ( $475\text{ M}^{-1}$ ). When the second amphiphile was replaced with a pyridine amphiphile ( $2C_{18}Py$ ) or with an alcohol amphiphile ( $2C_{18}OH$ ), binding constants for GlyLeu were lowered to 124 and  $43\text{ M}^{-1}$ , respectively. The enhanced binding in the former is attributed to strong guanidinium–carboxylate interaction upon C-terminal guest insertion and stable antiparallel hydrogen bonding among peptide chains. The binding of a second dipeptide, LeuGly, to the mixed monolayer of  $2C_{18}BGly_2NH_2/2C_{18}BGua$  gave a  $K$  value ( $2170\text{ M}^{-1}$ ) that is only one-third of that of GlyLeu. The difference is apparently related to the disposition of the hydrophobic side chain of the Leu residue in the C-terminal insertion. Thus, size matching of side chains of amino acid residues in host and guest determines selectivity of binding. Guest dipeptides are bound to the host most efficiently when the separation of host peptide chains is suited for the formation of strong hydrogen bonds between host and guest.

## Introduction

Molecular recognition of signal peptides by receptor proteins is a basic element in many biological events.<sup>1–3</sup> A large variety of artificial receptors have been developed in homogeneous solutions in order to mimic this process.<sup>4–6</sup> However, these artificial receptors do not incorporate the interfacial features characteristic of some biological recognition systems. There are a few examples of peptide-related binding sites that are incorporated into lipid monolayers. Higashi et al. found that  $\alpha$ -amino acids were selectively bound to monolayers of poly(L-glutamic acid) derivatives.<sup>7</sup> Leiserowitz and co-workers reported selective crystal formation of amino acids on monolayers of alkyl amino acids.<sup>8</sup> We have investigated the molecular rec-

ognition of nucleotides,<sup>9</sup> sugars,<sup>10</sup> nucleic acid bases,<sup>11</sup> and amino acids<sup>12</sup> that is achieved through complementary hydrogen bonding with appropriately functionalized monolayers.

Binding motifs between peptide chains do not necessarily display fixed complementarity, unlike base pairs in nucleic acids. Peptide chains assume conformationally varied structures, and versatile receptor sites are created by conformational variation of peptide residues. This rich possibility has been hardly explored in artificial systems. Recently, we started to examine recognition of aqueous peptides by monolayers that possess oligopeptide moieties as polar headgroups.<sup>13,14</sup> Peptide binding was not detected by monolayers composed of oligoglycine headgroups and single alkyl chains, because binding of aqueous peptide guests is hindered due to strong interamphiphile hydrogen

<sup>†</sup> Permanent address: Graduate School of Materials Science, Nara Institute of Science and Technology (NAIST), 8916–5 Takayama, Ikoma, Nara 630-0101, Japan.

<sup>‡</sup> Permanent address: Department of Biology, Sichuan Tumor Institute and Hospital Southern Train Station, Chengdu 610041, People's Republic of China.

<sup>§</sup> Permanent address: Faculty of Engineering, Kyushu University, Fukuoka 812-8581, Japan.

(1) Germain, R. N.; Margulies, D. H. *Annu. Rev. Immunol.* **1993**, *11*, 403.

(2) Stern, L. J.; Brown, J. H.; Jardetzky, T. S.; Gorga, J. C.; Urban, R. G.; Strominger, J. L.; Wiley, D. C. *Nature* **1994**, *368*, 215.

(3) Tame, J. R. H.; Murshudov, G. N.; Dodson, E. J.; Neil, T. K.; Dodson, G. G.; Higgins, C. F.; Wilkinson, A. J. *Science* **1994**, *264*, 1578.

(4) (a) Borchert, A.; Still, W. C. *J. Am. Chem. Soc.* **1994**, *116*, 373.

(b) Torneiro, M.; Still, W. C. *J. Am. Chem. Soc.* **1995**, *117*, 5887.

(5) Albert, J. S.; Goodman, M. S.; Hamilton, A. D. *J. Am. Chem. Soc.* **1995**, *117*, 1143.

(6) Labrenz, S. R.; Kelly, J. W. *J. Am. Chem. Soc.* **1995**, *117*, 1655.

(7) Higashi, N.; Saitou, M.; Mihara, T.; Niwa, M. *J. Chem. Soc., Chem. Commun.* **1995**, 2119.

(8) (a) Gidalevitz, D.; Weissbuch, I.; Kjaer, K.; Als-Nielsen, J.; Leiserowitz, L. *J. Am. Chem. Soc.* **1994**, *116*, 3271. (b) Landau, E. M.; Grayer Wolf, S.; Levanon, M.; Leiserowitz, L.; Lahav, M.; Sagiv, J. *J. Am. Chem. Soc.* **1989**, *111*, 1436.

(9) (a) Sasaki, D. Y.; Kurihara, K.; Kunitake, T. *J. Am. Chem. Soc.* **1991**, *113*, 9685. (b) Sasaki, D. Y.; Kurihara, K.; Kunitake, T. *J. Am. Chem. Soc.* **1992**, *114*, 10994. (c) Sasaki, D. Y.; Yanagi, M.; Kurihara, K.; Kunitake, T. *Thin Solid Films* **1992**, *210/211*, 776.

(10) (a) Kurihara, K.; Ohto, K.; Tanaka, Y.; Aoyama, Y.; Kunitake, T. *Thin Solid Films* **1989**, *179*, 21. (b) Kurihara, K.; Ohto, K.; Tanaka, Y.; Aoyama, Y.; Kunitake, T. *J. Am. Chem. Soc.* **1991**, *113*, 444.

(11) (a) Kurihara, K.; Ohto, K.; Honda, Y.; Kunitake, T. *J. Am. Chem. Soc.* **1991**, *113*, 5077. (b) Kawahara, T.; Kurihara, K.; Kunitake, T. *Chem. Lett.* **1992**, 1839.

(12) Ikeura, Y.; Kurihara, K.; Kunitake, T. *J. Am. Chem. Soc.* **1991**, *113*, 7342.

(13) Cha, X.; Ariga, K.; Onda, M.; Kunitake, T. *J. Am. Chem. Soc.* **1995**, *117*, 11833.

(14) (a) Cha, X.; Ariga, K.; Kunitake, T. *Chem. Lett.* **1996**, 73. (b) Cha, X.; Ariga, K.; Kunitake, T. *J. Am. Chem. Soc.* **1996**, *118*, 9545.







**2C<sub>18</sub>BValGlyNH<sub>2</sub>.** 2C<sub>18</sub>BValOH (525 mg, 0.660 mmol) was dissolved in CH<sub>2</sub>Cl<sub>2</sub> (30 mL), and DEPC (0.150 mL, 0.989 mmol) was added to the solution. After stirring at room temperature for 10 min, glycineamide hydrochloride (85.6 mg, 0.774 mmol) and triethylamine (0.300 mL, 2.15 mmol) dissolved in dry DMF (20 mL) were added. The mixture was allowed to react at room temperature for 50 h. CHCl<sub>3</sub> was added to the solution, which was then washed with water five times. After being dried over Na<sub>2</sub>SO<sub>4</sub>, the solvent was removed under reduced pressure. The residue was chromatographed on SiO<sub>2</sub> (1:1 CHCl<sub>3</sub>/acetone) to give 2C<sub>18</sub>BValGlyNH<sub>2</sub> as a white solid (365 mg, 67%): mp 106.0–126.5–127.0 °C (the arrow denotes liquid crystalline phases); TLC *R<sub>f</sub>* 0.4 (1:1 CHCl<sub>3</sub>/acetone); <sup>1</sup>H NMR (CDCl<sub>3</sub>) δ 0.88 (t, *J* = 6.3 Hz, 6H, 2 CH<sub>3</sub> in C<sub>18</sub> chain), 1.03 (t, *J* = 6.6 Hz, 3H, CH<sub>3</sub> in Val), 1.07 (t, *J* = 6.6 Hz, 3H, CH<sub>3</sub> in Val), 1.25 (br, 60H, 30 CH<sub>2</sub> in C<sub>18</sub> chain), 1.46–1.67 (br, 4H, 2 NCH<sub>2</sub>CH<sub>2</sub>), 2.34 (m, 1H, β-CH in Val), 3.12 (br, 2H, NCH<sub>2</sub>), 3.45 (br, 2H, NCH<sub>2</sub>), 3.70–3.97 (m, 2H, CH<sub>2</sub> in Gly), 4.32 (t, *J* = 7.7 Hz, 1H, α-CH in Val), 5.71 (br, 1H, NH), 6.66 (br, 1H, NH), 7.05 (br, 1H, NH), 7.32 (br, 1H, NH), 7.37 (d, *J* = 8.0 Hz, 2H, aromatic), 7.77 (d, *J* = 8.0 Hz, 2H, aromatic). Anal. Calcd for C<sub>51</sub>H<sub>92</sub>N<sub>4</sub>O<sub>4</sub>: C, 74.22; H, 11.24; N, 6.79. Found: C, 73.96; H, 11.26; N, 6.57.

**2C<sub>18</sub>BNO<sub>2</sub>.** Dioctadecylamine (370 mg, 0.709 mmol) was dissolved in hot CH<sub>2</sub>Cl<sub>2</sub> (100 mL), and triethylamine (0.150 mL, 1.08 mmol) and 4-nitrobenzoyl chloride (**1**) (171 mg, 0.923 mmol) were added to the solution. After being stirred for 3 h at room temperature, the organic layer was washed by NaHCO<sub>3</sub>(aq) and water and dried over Na<sub>2</sub>SO<sub>4</sub>, and the solvent was removed in vacuo. Recrystallization of the obtained residue from ethanol (50 mL) gave the title compound as colorless crystals (310 mg, 66%): mp 41.0–41.5 °C; <sup>1</sup>H NMR (CDCl<sub>3</sub>) δ 0.88 (t, *J* = 6.7 Hz, 6H, 2 CH<sub>3</sub>), 1.26 (br, 60H, 30 CH<sub>2</sub>), 1.56 (br, 4H, 2 NCH<sub>2</sub>CH<sub>2</sub>), 3.12 (t, *J* = 7.7 Hz, 2H, NCH<sub>2</sub>), 3.47 (t, *J* = 7.4 Hz, 2H, NCH<sub>2</sub>), 7.51 (d, *J* = 8.7 Hz, 2H, aromatic), 8.27 (d, *J* = 8.8 Hz, 2H, aromatic). Anal. Calcd for C<sub>43</sub>H<sub>78</sub>N<sub>2</sub>O<sub>3</sub>·1/4H<sub>2</sub>O: C, 76.45; H, 11.71; N, 4.15. Found: C, 76.49; H, 11.58; N, 4.15.

**2C<sub>18</sub>BNH<sub>2</sub>.** Pd/C (Pd 5%, 27 mg) and 2C<sub>18</sub>BNO<sub>2</sub> (234 mg, 0.349 mmol) were dispersed in THF (20 mL). The reaction mixture was kept under H<sub>2</sub> gas atmosphere at room temperature for 21 h. After filtration, the solvent was removed in vacuo. The title compound was obtained as a white solid (199 mg, 89%): mp 63.5–64.0 °C; <sup>1</sup>H NMR (CDCl<sub>3</sub>) δ 0.88 (t, *J* = 6.6 Hz, 6H, 2 CH<sub>3</sub>), 1.25 (br, 62H, 30 CH<sub>2</sub> + NH<sub>2</sub>), 1.56 (br, 4H, 2 NCH<sub>2</sub>CH<sub>2</sub>), 3.34 (br, 4H, 2 NCH<sub>2</sub>), 6.64 (d, *J* = 8.3 Hz, 2H, aromatic), 7.20 (d, *J* = 8.4 Hz, 2H, aromatic). Anal. Calcd for C<sub>43</sub>H<sub>80</sub>N<sub>2</sub>O: C, 80.56; H, 12.58; N, 4.37. Found: C, 80.34; H, 12.49; N, 4.28.

**2C<sub>18</sub>BGB.** A solution of 2C<sub>18</sub>BNH<sub>2</sub> (116 mg, 0.182 mmol) and 3,5-dimethylpyrazole-1-[*N,N*-bis(*tert*-butoxycarbonyl)]carboxamide (61.6 mg, 0.182 mmol) in CHCl<sub>3</sub> (5 mL) was allowed to react at 35 °C for 127 h. The mixture was concentrated under reduced pressure, and the residue was chromatographed on SiO<sub>2</sub> (4:1 hexane/EtOAc) to give 2C<sub>18</sub>BGB as a white solid (108 mg, 68%): mp 51.5–53.5–54.0 °C (the arrow denotes liquid crystalline phases); TLC *R<sub>f</sub>* 0.4 (4:1 hexane/EtOAc); <sup>1</sup>H NMR (CDCl<sub>3</sub>) δ 0.88 (t, *J* = 6.6 Hz, 6H, 2 CH<sub>3</sub> in C<sub>18</sub> chain), 1.25 (br, 60H, 30 CH<sub>2</sub>), 1.51 (s, 9H, 3 CH<sub>3</sub> in *t*-C<sub>4</sub>H<sub>9</sub>), 1.54 (s, 9H, 3 CH<sub>3</sub> in *t*-C<sub>4</sub>H<sub>9</sub>), 1.62 (br, 4H, 2 NCH<sub>2</sub>CH<sub>2</sub>), 3.21 (br, 2H, NCH<sub>2</sub>), 3.45 (br, 2H, NCH<sub>2</sub>), 7.33 (d, *J* = 8.7 Hz, 2H, aromatic), 7.66 (d, *J* = 8.4 Hz, 2H, aromatic), 10.48 (br, 1H, NH), 11.65 (br, 1H, NH). Anal. Calcd for C<sub>54</sub>H<sub>98</sub>N<sub>4</sub>O<sub>5</sub>: C, 73.42; H, 11.18; N, 6.34. Found: C, 73.50; H, 11.15; N, 6.33.

**2C<sub>18</sub>BGua.** A solution of 2C<sub>18</sub>BGB (90.7 mg, 0.103 mmol) in CH<sub>2</sub>Cl<sub>2</sub> (2 mL) and trifluoroacetic acid (TFA, 2 mL) was allowed to react at room temperature for 24 h. After the solvents were removed under reduced pressure, recrystallization of the residue from acetonitrile (20 mL) gave 2C<sub>18</sub>BG as a white solid (72.6 mg, 93%): mp 90.5–91.0 °C; <sup>1</sup>H NMR (CDCl<sub>3</sub>) δ 0.88 (t, *J* = 6.5 Hz, 6H, 2 CH<sub>3</sub>), 1.25 (br, 60H, 30 CH<sub>2</sub>), 1.51–1.66 (br, 4H, 2 NCH<sub>2</sub>CH<sub>2</sub>), 3.19 (br, 2H, NCH<sub>2</sub>), 3.47 (br, 2H, NCH<sub>2</sub>), 7.24–7.37 [br, 8H, aromatic (4H) + 2 NH<sub>2</sub>], 10.15 (s, 1H, NH). Anal. Calcd for C<sub>46</sub>H<sub>83</sub>N<sub>4</sub>O<sub>3</sub>F<sub>3</sub>: C, 69.31; H, 10.49; N, 7.03. Found: C, 69.27; H, 10.47; N, 6.99.

**C<sub>18</sub>BNO<sub>2</sub>.** Octadecylamine (1.26 g, 4.67 mmol) and triethylamine (1.00 mL, 7.17 mmol) were dissolved in CH<sub>2</sub>Cl<sub>2</sub> (150 mL), and *p*-nitrobenzoyl chloride (1.27 g, 6.51 mmol) was added to the solution. The mixture was allowed to react at room temperature

for 22 h, followed by washing with aqueous NaHCO<sub>3</sub>. After being dried over Na<sub>2</sub>SO<sub>4</sub>, the solvent was removed under reduced pressure. The residue was recrystallized from ethanol (200 mL) to give C<sub>18</sub>BNO<sub>2</sub> as a pale yellow solid (1.75 g, 90%): mp 109.0–109.5 °C; TLC *R<sub>f</sub>* 0.4 (3:1 hexane/EtOAc); <sup>1</sup>H NMR (CDCl<sub>3</sub>) δ 0.88 (t, *J* = 6.7 Hz, 3H, CH<sub>3</sub>), 1.25 (br, 30H, 15 CH<sub>2</sub>), 1.64 (m, 2H, NCH<sub>2</sub>CH<sub>2</sub>), 3.48 (q, *J* = 6.8 Hz, 2H, NCH<sub>2</sub>), 6.16 (br, 1H, NH), 7.92 (d, *J* = 7.9 Hz, 2H, aromatic), 8.29 (d, *J* = 7.8 Hz, 2H, aromatic). Anal. Calcd for C<sub>25</sub>H<sub>42</sub>N<sub>2</sub>O<sub>3</sub>: C, 71.73; H, 10.11; N, 6.69. Found: C, 71.73; H, 10.07; N, 6.64.

**C<sub>18</sub>BNH<sub>2</sub>.** Pd/C (Pd 10%, 189 mg) and C<sub>18</sub>BNO<sub>2</sub> (1.69 g, 4.04 mmol) were dispersed in THF (100 mL) and ethanol (30 mL). The reaction mixture was kept under H<sub>2</sub> gas atmosphere at room temperature for 71 h. The residue was recrystallized from acetonitrile (250 mL) to give C<sub>18</sub>BNH<sub>2</sub> as a white solid (1.12 g, 71%): mp 129.5–130.0 °C; <sup>1</sup>H NMR (CDCl<sub>3</sub>) δ 0.88 (t, *J* = 6.6 Hz, 3H, CH<sub>3</sub>), 1.26 (br, 30H, 15 CH<sub>2</sub>), 1.59 (m, 2H, NCH<sub>2</sub>CH<sub>2</sub>), 3.41 (q, *J* = 6.7 Hz, 2H, NCH<sub>2</sub>), 3.91 (br, 2H, NH<sub>2</sub>), 5.93 (br, 1H, NH), 6.65 (d, *J* = 7.6 Hz, 2H, aromatic), 7.59 (d, *J* = 7.6 Hz, 2H, aromatic). Anal. Calcd for C<sub>25</sub>H<sub>44</sub>N<sub>2</sub>O: C, 77.26; H, 11.41; N, 7.21. Found: C, 77.21; H, 11.36; N, 7.14.

**C<sub>18</sub>BGB.** C<sub>18</sub>BNH<sub>2</sub> (431 mg, 1.11 mmol) and **2** (377 mg, 1.11 mmol) in CHCl<sub>3</sub> (15 mL) were allowed to react at 35 °C for 330 h. The mixture was concentrated under reduced pressure, and the residue was chromatographed on SiO<sub>2</sub> (4:1 hexane/EtOAc) to give C<sub>18</sub>BGB as a white solid (470 mg, 67%): mp 98.5–99.0 °C; TLC *R<sub>f</sub>* 0.3 (4:1 hexane/EtOAc); <sup>1</sup>H NMR (CDCl<sub>3</sub>) δ 0.88 (t, *J* = 6.6 Hz, 3H, CH<sub>3</sub>), 1.25 (br, 30H, 15 CH<sub>2</sub>), 1.51 (s, 9H, *t*-C<sub>4</sub>H<sub>9</sub>), 1.54 (s, 9H, *t*-C<sub>4</sub>H<sub>9</sub>), 1.60 (m, 2H, NCH<sub>2</sub>CH<sub>2</sub>), 3.42 (q, *J* = 6.7 Hz, 2H, NCH<sub>2</sub>), 6.08 (br, 1H, NH in amide), 7.71 (m, 4H, aromatic), 10.50 (s, 1H, NH in guanidine), 11.62 (s, 1H, NH in guanidine). Anal. Calcd for C<sub>36</sub>H<sub>62</sub>N<sub>4</sub>O<sub>5</sub>·1/2H<sub>2</sub>O: C, 67.57; H, 9.92; N, 8.76. Found: C, 67.56; H, 9.75; N, 8.72.

**C<sub>18</sub>BGua.** A solution of C<sub>18</sub>BGB (435 mg, 0.689 mmol) in CH<sub>2</sub>Cl<sub>2</sub> (10 mL) and TFA (10 mL) was kept at room temperature for 20 h. After the solvents were removed under reduced pressure, the residue was recrystallized from acetonitrile (20 mL) to give C<sub>18</sub>BGua as a white solid (278 mg, 74%): mp 139.0–139.5 °C; <sup>1</sup>H NMR (DMSO-*d*<sub>6</sub>) δ 0.85 (t, *J* = 6.8 Hz, 3H, CH<sub>3</sub>), 1.23 (br, 30H, 15 CH<sub>2</sub>), 1.50 (m, 2H, NCH<sub>2</sub>CH<sub>2</sub>), 3.24 (q, *J* = 6.5 Hz, 2H, NCH<sub>2</sub>), 7.29 (d, *J* = 8.7 Hz, 2H, aromatic), 7.67 (br, 4H, 2 NH<sub>2</sub> in guanidinium), 7.90 (d, *J* = 8.7 Hz, 2H, aromatic), 8.47 (t, *J* = 5.6 Hz, 1H, NH in amide), 10.09 (br, 1H, NH in guanidinium). Anal. Calcd for C<sub>28</sub>H<sub>47</sub>N<sub>4</sub>O<sub>3</sub>F<sub>3</sub>: C, 61.74; H, 8.70; N, 10.29. Found: C, 61.68; H, 8.68; N, 10.25.

**2C<sub>18</sub>Py.** 4-Pyridinecarboxylic acid (**3**) (31 mg, 0.25 mmol) was dissolved in CH<sub>2</sub>Cl<sub>2</sub> (50 mL) and dry DMF (50 mL), and diethyl phosphorocyanidate (0.065 mL, 0.43 mmol) was added to the solution at 0 °C. After 15 min had passed, dioctadecylamine (0.099 g, 0.19 mmol) and triethylamine (0.120 mL, 0.86 mmol) dissolved in CH<sub>2</sub>Cl<sub>2</sub> (100 mL) were added to the acid solution at 0 °C. The reaction mixture was allowed to react at room temperature for 118 h. After the solvents were removed under reduced pressure, the residue was chromatographed on SiO<sub>2</sub> (1:1 hexane/EtOAc) to give 2C<sub>18</sub>Py (73 mg, 61%) as a white solid: mp 60.5–61.0 °C; TLC *R<sub>f</sub>* 0.5 (1:1 hexane/EtOAc); <sup>1</sup>H NMR (CDCl<sub>3</sub>) δ 0.88 (6H, t, *J* = 6.6 Hz, 2 CH<sub>3</sub>), 1.26 (60H, br, 30 CH<sub>2</sub>), 1.59 (4H, br, 2 NCH<sub>2</sub>CH<sub>2</sub>), 3.11 (2H, t, *J* = 7.6 Hz, NCH<sub>2</sub>), 3.47 (2H, t, *J* = 7.7 Hz, NCH<sub>2</sub>), 7.24 (2H, d, *J* = 6.0 Hz, aromatic), 8.67 (2H, d, *J* = 5.8 Hz, aromatic). Anal. Calcd for C<sub>42</sub>H<sub>78</sub>N<sub>2</sub>O: C, 80.44; H, 12.54; N, 4.47. Found: C, 80.19; H, 12.39; N, 4.38.

**Surface Pressure–Area (π–A) Isotherms.** π–A isotherms were measured with a computer-controlled film balance system FSD-50 (USI System, Fukuoka). A mixture of benzene/ethanol (80/20) was used as a spreading solvent. Equimolar, mixed monolayers were prepared by mixing separate solutions of each component. The starting trough area was 350.8 × 100.0 mm<sup>2</sup>, and 100 μL of the mixed solution was spread. Compression was started about 10 min after spreading at a rate of 0.2 mm·s<sup>−1</sup> (or 20 mm<sup>2</sup>·s<sup>−1</sup> based on area). The subphase temperature was kept at 20 ± 0.2 °C. The surface pressures were measured by a Wilhelmy plate, which was calibrated with the transition pressure of an octadecanoic acid monolayer.

**LB Films.** A gold-deposited slide glass was used as a substrate for LB transfer in order to measure reflection–absorption FT-IR spectra. It was prepared as follows. Glass slides (precleaned, 176

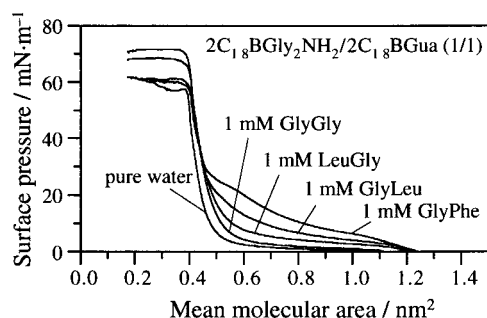


**Figure 1.**  $\pi$ -A isotherms of  $2C_{18}BGly_2NH_2/2C_{18}BGua$  (1/1) mixed monolayer on pure water and on 1 mM aqueous dipeptides (GlyGly, GlyLeu, LeuGly, and GlyPhe) at 20 °C.

$\times 26 \times 1 \text{ mm}^3$ , Iwaki Glass) were immersed in a detergent solution overnight (Dsn90, Bokusui Brown Co., Ltd.). The glass was washed with a large excess of ion-exchanged water to remove the detergent completely and subjected to sonication in fresh ion-exchanged water several times. After the glass was dried under vacuum for 1 h, chromium and gold thin layers were consecutively formed by the vapor-deposition method (1000 Å Au/50 Å Cr/slide glass) with a vapor-deposition apparatus VPC-260 (ULVAC Kyushu). Monolayers were transferred onto gold-deposited glass slides in the vertical mode at a surface pressure of 40  $\text{mN}\cdot\text{m}^{-1}$  for  $2C_{18}BGly_2NH_2$  and  $2C_{18}BGua$  monolayers and 35  $\text{mN}\cdot\text{m}^{-1}$  for the other monolayers. Dipping speeds of the plate were 5 and 20  $\text{mm}\cdot\text{min}^{-1}$  at up- and downstroke motions, respectively. Transfer ratio is almost unity in Y mode.

**FT-IR Measurements.** Infrared spectra of the LB film on gold-deposited glass were obtained on an FT-IR spectrometer (Nicolet 710) equipped with a MCT detector. All data were collected in the reflection absorption spectral (RAS) mode at a spectral resolution of 4  $\text{cm}^{-1}$ .

**Determination of Bound Guest by XPS Measurement.** X-ray photoelectron spectra (XPS) of LB films on gold-deposited glass were measured with a Perkin-Elmer PHI 5300 ESCA instrument (X-ray source Mg K $\alpha$  300 W, scan range 0–1000 eV, takeoff angle 45°). The elemental composition was obtained by dividing the observed peak area by intrinsic sensitivity factors of each element.

The amount of bound guest per amphiphile ( $y$ ) was calculated from the difference in the nitrogen/carbon ratio between the corresponding films and the film transferred from pure water, taking into account depth correction.<sup>19</sup> The  $y$  values were calculated for the total moles of the amphiphiles in the case of mixed monolayers. At least three separate runs were repeated under given conditions, and the obtained values were averaged. Error was estimated from their standard deviations. The  $y$  values were plotted as a function of guest concentration in the subphase, and the obtained plots were analyzed by curve fitting with the Langmuir equation (eq 1) in order to determine the binding constant ( $K$ ) and the binding ratio at saturation ( $\alpha$ ).

$$y = \alpha[\text{guest}]/(1/K + [\text{guest}]) \quad (1)$$

## Results and Discussion

**$\pi$ -A Isotherms of Equimolar  $2C_{18}BGly_2NH_2/2C_{18}BGua$  Monolayer on Aqueous Dipeptides.** We used four dipeptides, GlyGly, GlyPhe, GlyLeu, and LeuGly, to investigate the influences of the mode of insertion and peptide structure on the binding behavior. They have different side-chain sizes and peptide sequences.  $\pi$ -A isotherms are shown in Figure 1 for equimolar mixed monolayers of  $2C_{18}BGly_2NH_2/2C_{18}BGua$  on pure water and on 1 mM aqueous guests (GlyGly, GlyLeu, LeuGly, and GlyPhe). The abscissa represents average areas per one amphiphilic molecule. All of the isotherms show condensed phases with identical molecular areas of ca. 0.5  $\text{nm}^2$  at

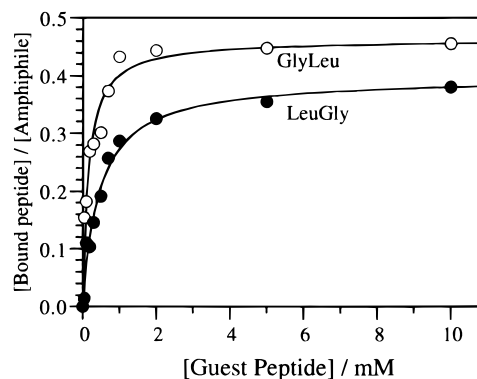


**Figure 2.** Binding of GlyLeu and LeuGly to  $2C_{18}BGly_2NH_2/2C_{18}BGua$  (1/1) mixed monolayer at 20 °C and 35  $\text{mN}\cdot\text{m}^{-1}$ . Amounts of bound guest per amphiphile molecule are plotted against guest concentrations in subphase.

high surface pressures, indicating that well-packed monomolecular layers were formed by compression. The presence of guest molecules in the subphase expanded isotherms in all cases. Effects of guest molecules were varied at lower pressure regions. A large dipeptide like GlyPhe tends to expand a monolayer. Expansion of monolayers at 20  $\text{mN}\cdot\text{m}^{-1}$  increases in the order of GlyPhe > GlyLeu > LeuGly > GlyGly. These behaviors may be caused by different modes or extents of substrate binding or both.

**Quantitative Analysis of the Binding of GlyLeu and LeuGly.** Binding of aqueous GlyLeu and LeuGly to an equimolar monolayer of  $2C_{18}BGly_2NH_2/2C_{18}BGua$  was evaluated quantitatively through XPS elemental analysis for LB films transferred on Au-deposited slide glasses. The amount of bound guest per amphiphile molecule was calculated from the nitrogen/carbon ratio upon depth correction from the film surface.<sup>19</sup> The extent of guest binding per monolayer component is shown against guest concentration in Figure 2. The binding is clearly saturated at high guest concentrations, in agreement with the formation of specific binding sites. Binding of GlyLeu reached saturation at ca. 1 mM, but saturation for LeuGly was observed at higher concentrations. The amount of bound guests at saturation was larger for GlyLeu than for LeuGly.

Fitting of the binding curve to the Langmuir isotherm gave binding constant ( $K$ ) and saturation binding ratio ( $\alpha$ , guest/amphiphile ratio at saturation binding). These data are summarized in Table 1 together with related data. The  $\alpha$  values for GlyLeu and LeuGly are close to 0.5 and 0.4, respectively. It is thus indicated, as in our previous study,<sup>14</sup> that one molecule each of the two monolayer components is involved in the binding of one guest molecule. However, this does not mean that the binding interaction of the guest dipeptides is limited to one molecule each of the two monolayer components. It is more likely, as will be discussed later, that monolayer components, especially the peptide component, can interact with multiple guest molecules simultaneously by forming a regular molecular lattice. The  $\alpha$  value of 0.4 observed for the LeuGly guest is difficult to explain. It is possible that the molecular lattice of the receptor monolayer becomes partially irregular to lose full binding capability toward LeuGly.

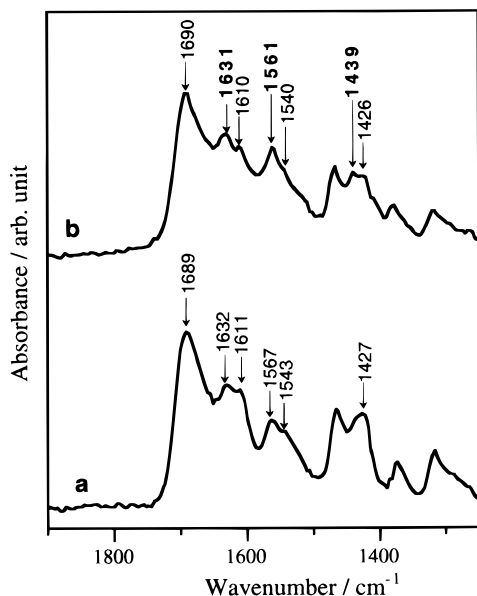
The binding constant is much larger when the guanidinium function is included as the second component in place of the carboxylate function. This is readily expected from stronger interaction of the guanidinium ion with the carboxylate function.

(19) Kurihara, K.; Kawahara, T.; Sasaki, D. Y.; Ohto, K.; Kunitake, T. *Langmuir* **1995**, *11*, 1408.



**Table 1. Binding Constant ( $K$ ) and Saturation Binding Ratio ( $\alpha$ ) of Peptide Binding to Various Monolayers**

monolayer	guest	$K/M^{-1}$	$\alpha$	remarks
$2C_{18}BGly_2NH_2$	GlyLeu	$35 \pm 6$	$1.33 \pm 0.09$	Cha et al. <sup>13</sup>
$2C_{18}BGly_2NH_2/2C_{18}BCOOH$ ( $1/1$ )	GlyLeu	$475 \pm 18$	$0.47 \pm 0.03$	Cha et al. <sup>14b</sup>
$2C_{18}BGly_2NH_2/2C_{18}BGua$ ( $1/1$ )	GlyLeu	$6400 \pm 1000$	$0.46 \pm 0.02$	this study
$2C_{18}BGly_2NH_2/2C_{18}BGua$ ( $1/1$ )	LeuGly	$2170 \pm 290$	$0.40 \pm 0.02$	this study
$2C_{18}BGly_2NH_2/2C_{18}Py$ ( $1/1$ )	GlyLeu	$124 \pm 19$	$0.59 \pm 0.03$	this study
$2C_{18}BGly_2NH_2/2C_{18}OH$ ( $1/1$ )	GlyLeu	$43 \pm 11$	$0.39 \pm 0.04$	this study

**Figure 3.** FT-IR spectra (RAS mode) of  $2C_{18}BGly_2NH_2/2C_{18}BGua$  ( $1/1$ ) LB films (10 layers) transferred from (a) pure water and (b) 10 mM GlyLeu at  $35 \text{ mN}\cdot\text{m}^{-1}$ .

**FT-IR Study of the Binding Mode of GlyLeu to the Peptide/Guanidinium Monolayer.** The XPS results indicate binding of GlyLeu and LeuGly to the mixed monolayer. We previously found very strong interaction of guanidinium functions with aqueous phosphate (binding constant is more than  $10^6 \text{ M}^{-1}$ )<sup>9</sup> and with aqueous carboxylate (binding saturation at  $10^{-4} \text{ M}$  of the guest)<sup>17</sup> at the air–water interface. Therefore, it is reasonable to assume that enhanced binding constants observed in the present study are originated in the strong interaction between guanidinium and the C-terminal of the guest dipeptides.

FT-IR measurements give information on the mode of host/guest binding. FTIR–RAS spectra were measured for  $2C_{18}BGly_2NH_2/2C_{18}BGua$  LB films (10 layer) transferred from pure water and aqueous 10 mM GlyLeu (Figure 3). Unfortunately, the strong host peaks at  $1400\text{--}1700 \text{ cm}^{-1}$  hinder detailed analysis of guest binding. New peaks due to bound GlyLeu,  $\delta(\text{CH}_3)$ , and amide II bands are seen at  $1439$  and  $1561 \text{ cm}^{-1}$ , respectively, from comparison of Figure 3a,b. Similar peaks have been observed for GlyLeu bound to a different monolayer receptor: The  $\delta(\text{CH}_3)$  peak was seen at  $1440 \text{ cm}^{-1}$  upon binding of GlyLeu to the  $2C_{18}BGly_2NH_2$  monolayer,<sup>13</sup> and amide II peaks were detected at  $1560$  and  $1559 \text{ cm}^{-1}$  upon binding of GlyLeu to the  $2C_{18}BGly_2NH_2$ <sup>13</sup> and  $2C_{18}BGlyValNH_2/2C_{18}BCOOH$ <sup>14b</sup> monolayers, respectively. Figure 3b does not contain a  $\delta(\text{NH}_3)$  peak, which has been found at  $1508 \text{ cm}^{-1}$  in a GlyLeu cast film.<sup>13</sup> This suggests that the N-terminal ammonium group of bound GlyLeu is hydrogen-bonded to the  $2C_{18}BGly_2NH_2/2C_{18}BGua$  monolayer. A similar observation was made for bound GlyLeu in a  $2C_{18}BGly_2NH_2$  cast film. The site of the hydrogen bond is probably the glycylglycinamide residue in the mixed monolayer.

Spectral features of the C-terminal COOH are summarized as follows. It is known that the  $\nu(\text{C=O})$  peak of unbound COOH and the  $\nu_a(\text{COO}^-)$  peak are present at  $1700\text{--}1730 \text{ cm}^{-1}$  and at around  $1600 \text{ cm}^{-1}$ , respectively. On the other hand, the  $\nu(\text{C=O})$  peak of the COOH group is observed at ca.  $1650 \text{ cm}^{-1}$  when it is hydrogen-bonded to guanidinium.<sup>17</sup> Brzezinski et al.<sup>20</sup> similarly found a  $\nu(\text{C=O})$  peak of COOH hydrogen-bonded to guanidinium with a large proton polarizability at  $1633 \text{ cm}^{-1}$ . The IR spectrum of Figure 3b does not have peaks of unbound COOH and  $\text{COO}^-$  and, instead, showed an enhanced peak intensity at  $1631 \text{ cm}^{-1}$  relative to that at  $1610 \text{ cm}^{-1}$ . This might be a combined effect of the presence of the COOH group hydrogen-bonded to guanidinium and the amide I band of bound GlyLeu.

**Influence of Second Receptor Functions on the Binding of GlyLeu Guest.** The effect of the second receptor function was subsequently examined for the binding of GlyLeu to equimolar mixed monolayers of  $2C_{18}BGly_2NH_2/2C_{18}Py$  and  $2C_{18}BGly_2NH_2/2C_{18}OH$ . Binding constants ( $K$ ) and saturation binding ratios ( $\alpha$ ) calculated from binding curves are collected in Table 1. The  $\alpha$  values for the  $2C_{18}BGly_2NH_2/2C_{18}Py$  and  $2C_{18}BGly_2NH_2/2C_{18}OH$  monolayers are 0.6 and 0.4, respectively, and are essentially identical to the guanidinium case. The  $\alpha$  value of 0.5 may be explained either by formation of cooperative binding sites with the  $2C_{18}BGly_2NH_2/2C_{18}BCOOH$  monolayer or by complete phase separation of the second, ineffective component. The latter possibility, however, can be denied because enhanced binding is observed. For example, the  $2C_{18}BGly_2NH_2/2C_{18}BCOOH$  monolayer shows an enhanced affinity toward GlyLeu compared with either of those of the single-component monolayers.<sup>14</sup>

Monolayers of  $2C_{18}BGly_2NH_2/2C_{18}Py$  give an enhanced binding constant ( $124 \text{ M}^{-1}$ ) compared with that of  $2C_{18}BGly_2NH_2$  monolayer ( $35 \text{ M}^{-1}$ ). FT-IR spectra of LB films of  $2C_{18}BGly_2NH_2/2C_{18}Py$  are shown in Figure 4. When the film was transferred from 10 mM GlyLeu subphase, amide I and II peaks of bound GlyLeu are seen at  $1629$  and  $1560 \text{ cm}^{-1}$ , respectively (Figure 4b). The  $\nu_a(\text{COO}^-)$  peak at ca.  $1600 \text{ cm}^{-1}$  was not observed and a new peak appeared at  $1691 \text{ cm}^{-1}$ . The latter peak is probably due to the  $\nu(\text{C=O})$  of weakly hydrogen-bonded COOH, indicating that the C-terminal of GlyLeu forms a hydrogen bond with pyridine rather than the salt bridge. When GlyLeu is bound to the monolayer by C-terminal insertion, antiparallel hydrogen bonding would be formed between peptide chains of the host and the guest and the Leu side chain becomes directed close to the air phase. This peptide interaction is similar to that presumed for the binding of GlyLeu to the  $2C_{18}BGly_2NH_2$  monolayer. The additional interaction between host pyridine and guest COOH increases the binding constant. However, the enhancement in this case is much smaller than that for  $2C_{18}BGly_2NH_2/2C_{18}BGua$ . This is a reflection of weaker interaction between the second monolayer component and the guest

(20) Brzezinski, B.; Olejnik, J.; Zundel, G. *J. Chem. Soc., Faraday Trans.* **1994**, *90*, 1095.

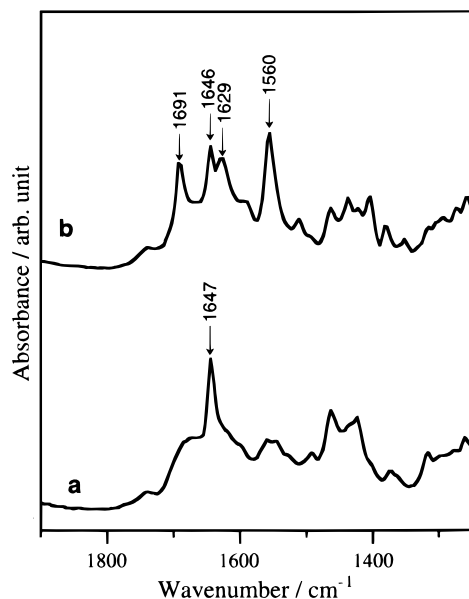


**Figure 4.** FT-IR spectra (RAS mode) of  $2C_{18}BGly_2NH_2/2C_{18}Py^{(1/1)}$  LB films (10 layers) transferred from (a) pure water and (b) 10 mM GlyLeu at  $35\text{ mN}\cdot\text{m}^{-1}$ .

terminal group. Guanidinium/carboxylate interaction is much stronger than pyridine-COOH hydrogen bonding.<sup>16,17</sup>

The observed binding constant of GlyLeu to the  $2C_{18}BGly_2NH_2/2C_{18}OH$  monolayer ( $43\text{ M}^{-1}$ ) is close to that for the  $2C_{18}BGly_2NH_2$  single-component monolayer. Therefore, the  $2C_{18}OH$  component may not contribute to guest binding.

**Selective Binding of Dipeptide Guests toward the Diglycyl-Guanidinium Monolayer.** In our previous studies on the binding of aqueous dipeptides to the single-component monolayer of  $2C_{18}BGly_2NH_2$  and to the mixed monolayer of  $2C_{18}BGly_2NH_2/2C_{18}BCOOH$ , we discussed binding selectivity on the basis of the assumption that C-terminal guest insertion is more stable because of formation of antiparallel hydrogen bonding. However, the mode of guest insertion was not necessarily clear. In the case of the single-component monolayer, clear evidence for the C-terminal insertion could not be presented.<sup>13</sup> Both C-terminal and N-terminal insertions were conceivable in the latter mixed monolayer,<sup>14b</sup> because both of the dipeptide terminals could interact with the COOH group of benzoic acid. Thus, two insertion modes had to be considered, and their discrimination was not easy. In contrast, the mixed monolayer of  $2C_{18}BGly_2NH_2/2C_{18}BGua$  can restrict the guest binding to the C-terminal insertion because of strong guanidinium-carboxylate interaction.

A plausible binding motif of GlyLeu to the  $2C_{18}BGly_2NH_2/2C_{18}BGua$  monolayer is depicted in Figure 5A. Hydrogen bonding between guanidinium ( $2C_{18}BGua$ ) and the C-terminal carboxylate of GlyLeu is formed, and the two kinds of amphiphiles form binding sites cooperatively in a 1:1 molar ratio. Stable antiparallel hydrogen bonding is formed between host and guest in this binding structure. Unfavorable contact between the Leu side chain and bulk water can be avoided. Contribution of these favorable interactions would produce a large binding constant ( $6400\text{ M}^{-1}$ ).

Because guanidinium/carboxylate interaction is quite strong, sequentially reversed LeuGly may also be inserted from the C-terminal (Figure 5B). In this motif, stable antiparallel hydrogen bonding is formed, but the Leu side chain that is located close to the N-terminal becomes

exposed to water, causing energetically unfavorable contact. This disadvantage apparently decreases the binding constant from  $6400\text{ (GlyLeu)}$  to  $2170\text{ M}^{-1}\text{ (LeuGly)}$ .

We compared the binding efficiency of GlyLeu and LeuGly toward different host monolayers (summarized in Figure 6). Binding of GlyLeu to the  $2C_{18}BGly_2NH_2/2C_{18}BGua$  monolayer is significantly greater than those to the corresponding single-component monolayers of  $2C_{18}BGly_2NH_2$  or  $2C_{18}BGua$ . This fact confirms that efficient binding site is created by the cooperative action of the two amphiphiles. We also examined the binding capability of a mixed monolayer host that includes monoalkyl guanidinium ( $2C_{18}BGly_2NH_2/C_{18}BGua$ ) (see Figure 7C for the  $\pi$ -A isotherms of  $2C_{18}BGly_2NH_2/C_{18}BGua$ ). The binding of GlyLeu to this monolayer (guest/host ratio of 0.35 at 1 mM GlyLeu as given in Figure 6) is less efficient than that to  $2C_{18}BGly_2NH_2/2C_{18}BGua$  (guest/host ratio of 0.44 at 1 mM GlyLeu). The use of the double-chain guanidinium provides a greater binding cavity. There must be an optimal cavity size that causes efficient hydrogen bonding between peptide chains of host and guest. Further investigation on the influence of cavity size is now in progress.

It is interesting to compare binding behavior of other dipeptide guests to that of the  $2C_{18}BGly_2NH_2/2C_{18}BGua$  monolayer. Among GlyGly, GlyLeu, and GlyPhe, stronger binding was observed when more hydrophobic residues were attached to the C-terminal residue. It must be hydrophobic interaction between the guest side chain and monolayers that promotes guest binding, because the C-terminal side chains are located close to the hydrophobic region of monolayer, as illustrated in Figure 5A. Binding of GlyPhe might also be enhanced by  $\pi$ - $\pi$  stacking with the terephthaloyl unit of amphiphiles.

**Binding Selectivity and Side-Chain Interaction between Receptor and Guest.** The nature of the binding cavity is influenced by the structure of host peptide units. This was tested by using peptide amphiphiles with Val residue,  $2C_{18}BGlyValNH_2$  and  $2C_{18}BValGlyNH_2$ .  $\pi$ -A isotherms of 1:1 mixtures of  $2C_{18}BGlyValNH_2/2C_{18}BGua$  and  $2C_{18}BValGlyNH_2/2C_{18}BGua$  are shown in Figure 7. The effect of the dipeptide guest on the isotherm is similar to that for  $2C_{18}BGly_2NH_2/2C_{18}BGua$ ; i.e., GlyPhe expanded the isotherm most efficiently and the smallest effect was observed with GlyGly.

The amount of GlyLeu and LeuGly bound to  $2C_{18}BGlyValNH_2/2C_{18}BGua$  and  $2C_{18}BValGlyNH_2/2C_{18}BGua$  monolayers was determined by XPS analysis of transferred LB films and is shown in Figure 6. The chemical composition of the two guests is identical, but their peptide sequences are reversed. The binding efficiencies are dependent on the chemical structures of both monolayer and guest. In the case of the  $2C_{18}BGlyValNH_2/2C_{18}BGua$  monolayer, the binding of GlyLeu is much greater than that of LeuGly. In contrast, these two guests are bound to the  $2C_{18}BValGlyNH_2/2C_{18}BGua$  monolayer at intermediate efficiencies. Assuming the C-terminal insertion is due to strong guanidinium/carboxylate interaction, binding motifs for the four cases can be depicted as in Figure 8. Hydrogen bonding is antiparallel in all cases. Therefore, the observed binding selectivity may be predominantly determined by the location and steric hindrance of side chains. In the binding of GlyLeu to the  $2C_{18}BGlyValNH_2/2C_{18}BGua$  monolayer, the isobutyl side chain of Leu is directed to the hydrophobic interior of the monolayer; and the steric hindrance of the Leu side chain with an amphiphile Val side chain should be absent (Figure 8A). These favorable factors induce the largest binding efficiency. In contrast, unfavorable contact of the hydro-



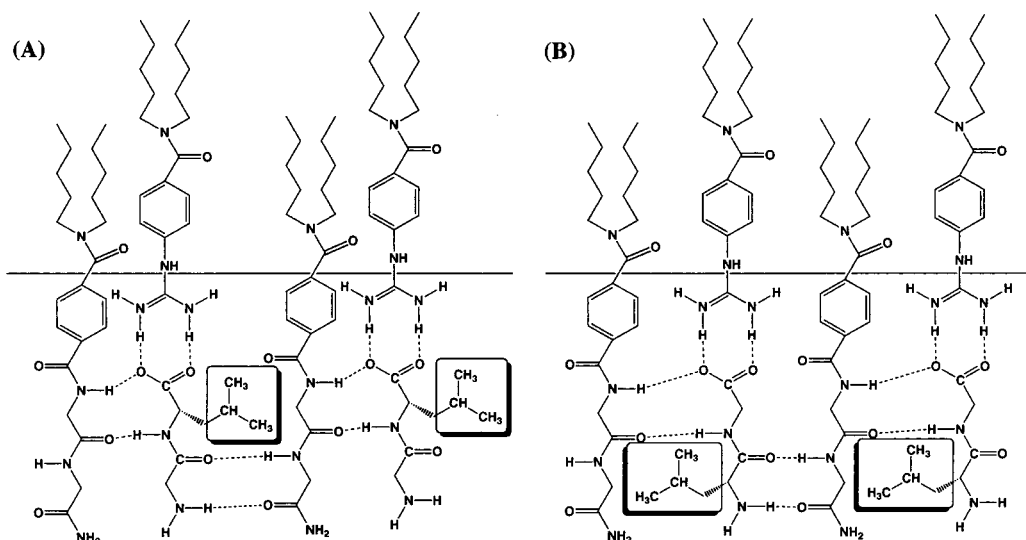


**Figure 5.** Plausible binding motifs of aqueous dipeptides to  $2C_{18}BGly_2NH_2/2C_{18}BGua$  ( $1/1$ ) mixed monolayer: A, GlyLeu guest, and B, LeuGly guest.

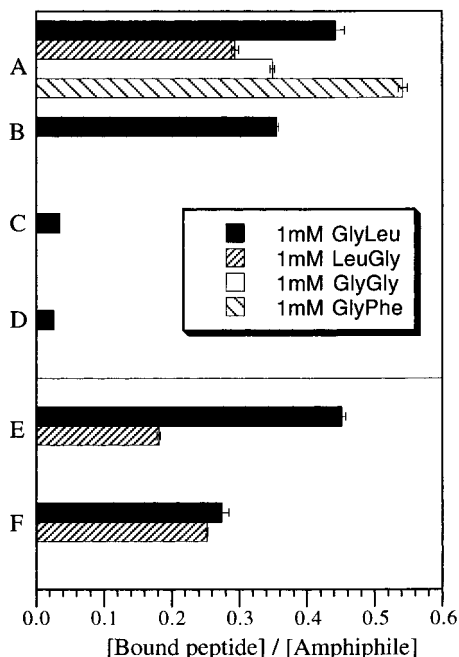


**Figure 6.** Amount of bound dipeptides (GlyGly, GlyLeu, LeuGly, and GlyPhe at 1 mM) to receptor monolayers at 20 °C: A,  $2C_{18}BGly_2NH_2/2C_{18}BGua$  ( $1/1$ ); B,  $2C_{18}BGly_2NH_2/2C_{18}BGua$  ( $1/1$ ); C,  $2C_{18}BGly_2NH_2$ ; D,  $2C_{18}BGua$ ; E,  $2C_{18}BGlyValNH_2/2C_{18}BGua$  ( $1/1$ ); and F,  $2C_{18}BValGlyNH_2/2C_{18}BGua$  ( $1/1$ ).

phobic chain of the guest with water and steric crowding between Leu and Val residues are conceivable for the binding of LeuGly to the same monolayer (Figure 8B). The guest binding is least efficient in this case. One of these two unfavorable factors is absent in the binding of GlyLeu to the  $2C_{18}BValGlyNH_2/2C_{18}BGua$  monolayer (Figure 8C), and of LeuGly to the  $2C_{18}BValGlyNH_2/2C_{18}BGua$  monolayer (Figure 8D). Thus, the latter two cases lead to intermediate binding efficiencies.

**Nature of Binding Site.** Among the host monolayers we investigated in this study, the one with the guanidinium component showed much larger binding constants. The binding constant of GlyLeu with the equimolar monolayer of  $2C_{18}BGly_2NH_2$  and  $2C_{18}BGua$  is  $6400\text{ M}^{-1}$ , whereas those with the single-component  $2C_{18}BGly_2NH_2$  monolayer<sup>13</sup> and an equimolar monolayer of  $2C_{18}BGly_2-$

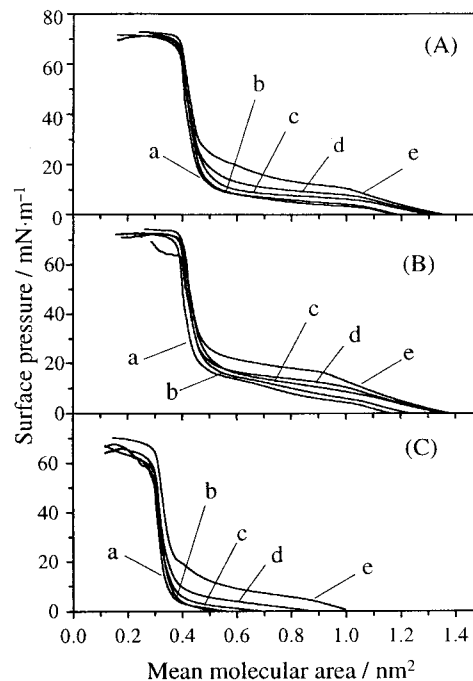


**Figure 7.**  $\pi$ -A isotherms of mixed monolayers on (a) pure water and on 1 mM aqueous dipeptides [(b) GlyGly, (c) LeuGly, (d) GlyLeu, and (e) GlyPhe] at 20 °C: A,  $2C_{18}BGlyValNH_2/2C_{18}BGua$  ( $1/1$ ); B,  $2C_{18}BValGlyNH_2/2C_{18}BGua$  ( $1/1$ ); and C,  $2C_{18}BGly_2NH_2/2C_{18}BGua$  ( $1/1$ ).

$NH_2$  and  $2C_{18}BCOOH$ <sup>14b</sup> are only  $35\text{ M}^{-1}$  and  $475\text{ M}^{-1}$ , respectively. Guanidinium is a strong base and is bound tightly to carboxylate through electrostatic attraction and hydrogen bonding.<sup>16,17</sup> This mode of the interaction is much stronger than the interaction of host COOH or pyridine with the C-terminal functional group of the guest. In fact, we observed very high binding constants of  $10^6$ – $10^7\text{ M}^{-1}$  between the guanidinium monolayer and aqueous phosphate.<sup>9</sup> The binding of guanidinium monolayers with aqueous carboxylates was similarly effective.<sup>17</sup>

However, guanidinium alone is not as effective as the mixed monolayer as seen from Figure 6. Cooperative action of the two monolayer components is crucial for the very strong binding observed. Guest dipeptides may exist in a zwitterionic form in water, and then, they are not

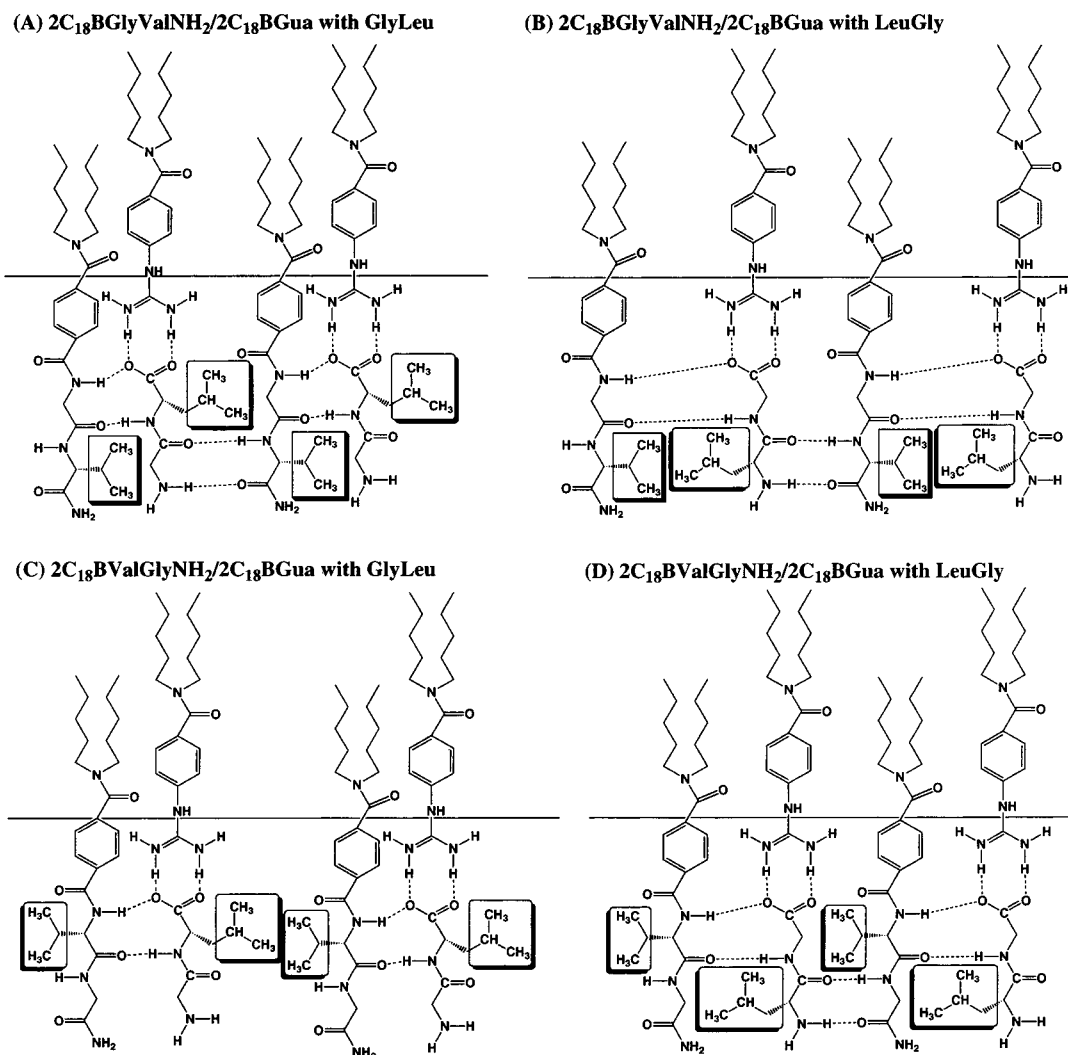


**Figure 8.** Plausible binding motifs of aqueous dipeptides to mixed monolayers.

efficiently bound to the guanidinium monolayer. The interaction between guanidinium (host) and carboxylate (guest) would be strengthened when guest dipeptides are inserted between host peptide residues with C-terminal fixation (see Figure 5A). Binding stoichiometry (ca. 0.5) and cooperative action of the two monolayer components strongly suggest the formation of an ordered superstructure for the host–guest complex. The binding model of Figure 5A, which is supported by FT-IR data, requires alternate arrangement of  $2C_{18}BGly_2NH_2$  and  $2C_{18}BGua$  molecules within monolayer. The binding stoichiometry of ca. 0.4 formed for LeuGly guest may indicate that the regular, alternative structure is only incompletely formed. Formation of a regular molecular arrangement upon guest binding has been confirmed for other monolayers based on atomic force microscopic (AFM) observation. A regular molecular pattern was induced in a mixed monolayer of guanidinium and orotate upon the binding of aqueous flavin adenine dinucleotide (FAD).<sup>18</sup> A melamine monolayer gave regular molecular packing through hydrogen bonding with aqueous barbituric acid.<sup>21</sup> Similarly, it is reasonable to assume that an alternate molecular arrangement is induced in the peptide/guanidinium monolayer through formation of multiple hydrogen bonds with peptide guest.

The spatial disposition of monolayer components is restricted to the 2D plane of the air–water interface, and the mode of molecular assembly at the receptor site is determined by packing and orientation of alkyl chains and interaction of neighboring functional moieties. Representative modes of molecular packing in the host monolayer are proposed in Figure 9. The guest dipeptides are bound to the guanidinium site. In these models, alkyl chains are packed hexagonally, peptide chains of host and guest are assumed to be extended to form hydrogen bonds between the two, and the guest dipeptide is positioned on guanidinium group. Linear networks of hydrogen bonding are produced as a result of the host/guest interaction, as one guest dipeptide forms hydrogen bonds with two host peptide chains. The distance between guest and host peptide chains and the separation between the neighboring hydrogen-bond networks are estimated as given in Figure 9 on the basis of the cross-sectional area of a single alkyl chain of  $0.2 \text{ nm}^2$ . Models a–e illustrate the guest-bound 2D structure of equimolar mixed monolayers of  $2C_{18}BXYNH_2/2C_{18}Gua$ . Because the total molecular area of host and guest is identical among these models, an increase in the distance between peptide chains of host and guest leads to a decrease in separation between extended hydrogen-bond networks. In models a and b, the host–guest distance and the separation between hydrogen-bond networks are 0.48 and 0.83 nm, respectively. The distance

(21) Koyano, H.; Yoshihara, K.; Ariga, K.; Kunitake, T.; Oishi, Y.; Kawano, O.; Kuramori, M.; Suehiro, K. *Chem. Commun.* **1996**, 184.

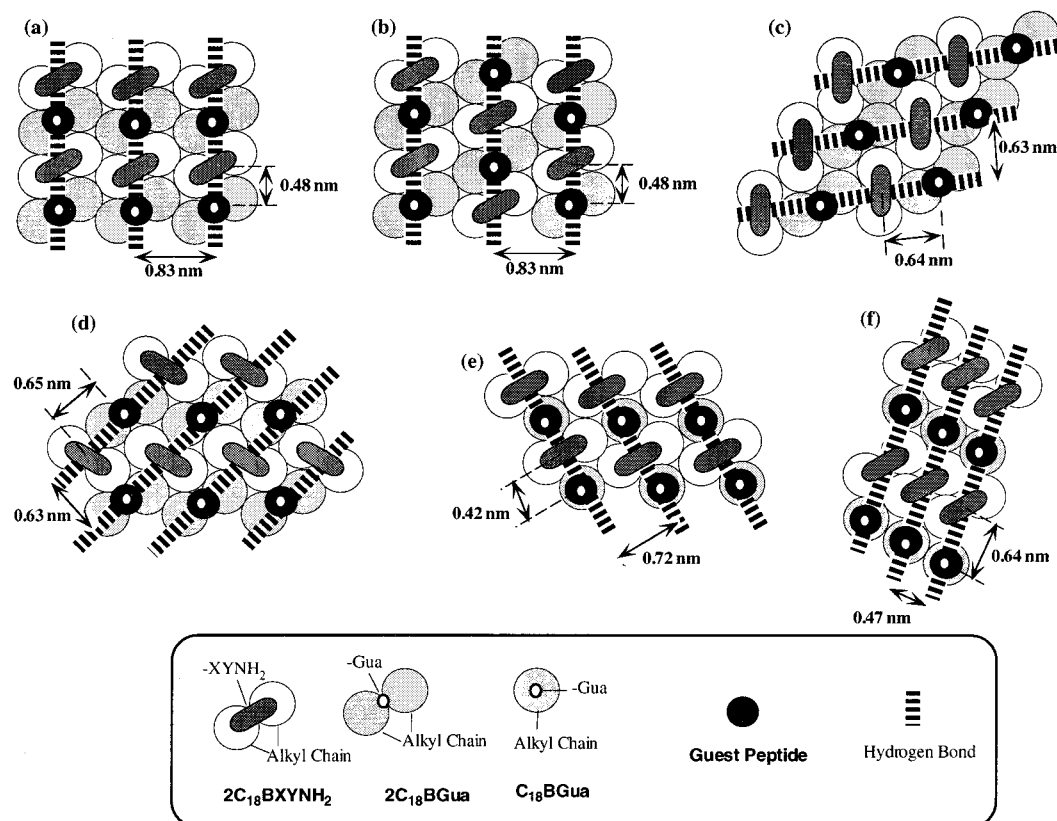


**Figure 9.** Two-dimensional models proposed for arrays of peptide binding sites as seen from the aqueous phase: (a)–(d), on  $2C_{18}BXYNH_2/2C_{18}BGua$  ( $1/1$ ) monolayer; (e) and (f),  $2C_{18}BXYNH_2/C_{18}BGua$  ( $1/1$ ) monolayer. GlyLeu guest is placed on the guanidinium function. The guanidinium functions should be hidden by bound GlyLeu in the view from aqueous phase, but we show them as open circles to indicate the position of the guanidinium functions. Alkyl chains are assumed to be packed hexagonally.

of peptide chains in antiparallel  $\beta$ -sheet has been reported as 0.47 nm.<sup>22,23</sup> Therefore, these models give good distance for hydrogen bonding between host and guest. Large separation between the neighboring hydrogen-bond networks is advantageous for avoiding steric hindrance between side chains of receptor and guest. These favorable geometrical conditions must contribute to the large binding constants of the  $2C_{18}BXYNH_2/2C_{18}Gua$  monolayers. In contrast, models c and d give a larger host–guest distance (0.65 nm) and a smaller separation between hydrogen-bond networks (0.72 nm). The larger host–guest distance is obviously less advantageous than those in models a and b in guest binding.

Accommodation of side chains of guest dipeptides in the binding site would be affected by the cavity size of the latter. The extended length of Val and Leu residues is in the range of 0.2–0.4 nm from the Corey–Pauling–Koltun model. The amino acid side chains of this size appear to be easily accommodated in the receptor cavity of models a–d.

Models e and f of Figure 9 show guest binding to the mixed monolayer of  $2C_{18}BXYNH_2$  and monoalkyl  $C_{18}Gua$ . The relative area occupied by the guest is decreased to  $3/4$  of that in  $2C_{18}BXYNH_2/2C_{18}Gua$  monolayer, and the host–guest distance and the separation between hydrogen-bond networks become smaller. Model e has a host–guest distance of 0.42 nm and separation between hydrogen-bond networks of 0.72 nm. The latter value is large enough to accommodate side chains, but the former value is smaller than the peptide distance appropriate for antiparallel  $\beta$ -sheet structure (0.47 nm). Model f has a larger

host–guest distance (0.64 nm) but a smaller separation (0.47 nm). These figures become larger if alkyl chains are tilted, and the corresponding receptor cavity can be large enough for accommodating guest dipeptides snugly. However, the binding efficiency for this monolayer is smaller than those for other monolayers (Figure 6), and a less favorable binding site must be formed.

We investigated separately the binding efficiency of a GlyLeu guest to single-component monolayers of oligoglycine amphiphiles with one, two, four, and six alkyl chains.<sup>24</sup> The most effective binding was observed for monolayers of dialkyl amphiphiles. Monoalkyl amphiphiles lead to formation of overly small cavities where strong hydrogen bonding among neighboring peptide chains prevents guest binding.<sup>15,24</sup> Receptor cavities formed by monolayers of tetra- and hexaalkyl amphiphiles were too large to achieve efficient guest binding.

The above discussion is based on a simple packing model of alkyl chains. In the actual system, the host–guest interaction may vary depending on the structure of guest dipeptides. This situation is reminiscent of the “induced-fit” mechanism proposed for enzyme catalysis by D. E. Koshland many years ago,<sup>25</sup> because monolayer components that surround the guest molecule will assume best-fit conformations. The first and the second amino acid residues could form hydrogen bonding in different directions, as seen in the polyglycine II structure, to achieve the best fit.<sup>26</sup>

(22) Bandekar, J. *Biochim. Biophys. Acta* **1992**, 1120, 123.

(23) Arnott, S.; Dover, S. D.; Elliott, A. *J. Mol. Biol.* **1967**, 30, 201.

(24) Koyano, H.; Ariga, K.; Kamino, A.; Kunitake, T., manuscript in preparation.

(25) Koshland, D. E., Jr.; Nemethy, G.; Filmer, D. *Biochemistry* **1971**, 10, 5.

(26) Crick, F. H. C.; Rich, A. *Nature* **1955**, 176, 780.

Size matching of side chains of host and guest peptides was noticed more clearly in our previous study on single-component peptide receptors where only  $2C_{18}BGly_2NH_2$  among the  $2C_{18}BGlyXNH_2$  possibilities ( $X = Gly, Ala, Val, Leu,$  and  $Phe$ ) showed affinity to aqueous  $GlyLeu$ .<sup>14b</sup> Side chains in the host amphiphile would suppress the cavity size. The binding efficiency was dependent on the size of side chains in mixed monolayers of  $2C_{18}BGlyXNH_2$  and  $2C_{18}BGly_2COOH$ .<sup>14b</sup> Guest dipeptides with bulky side chains such as  $GlyLeu$  showed higher binding affinities toward the  $2C_{18}BGly_2NH_2/2C_{18}BCOOH$  monolayer than toward the  $2C_{18}BGlyValNH_2/2C_{18}BCOOH$  monolayer. In contrast, the small  $GlyGly$  moiety is bound more efficiently to the  $2C_{18}BGlyValNH_2/2C_{18}BCOOH$  monolayer than to the  $2C_{18}BGly_2NH_2/2C_{18}BCOOH$  monolayer. These results show the importance of size matching of amino acid side chains between host and guest. Little steric hindrance and large van der Waals contact arising from the size matching would lead to enhanced peptide binding. As shown in Figure 8, guest insertion from the C-terminal is predominant because of strong guanidinium/carboxylate interaction. This factor produces a better size matching (highest binding efficiency) in binding of  $GlyLeu$  to the  $2C_{18}BGlyValNH_2/2C_{18}BGua$  monolayer (Figure 8A), but not for  $LeuGly$  to the same monolayer (Figure 8B).

### Conclusion and Future Prospects

Mixed monolayers of peptide and guanidinium amphiphiles incorporate aqueous dipeptides with binding constants greater than  $10^3 M^{-1}$  at the air–water interface. Molecularly defined binding sites would be induced by the self-assembly of component amphiphiles. Such binding sites are readily modified by selecting appropriate combinations of peptide and guanidinium amphiphiles.

The observed high efficiency of binding may lead to sensitive detection of aqueous peptides. This feature should be useful for designed sensing of physiologically important peptides such as peptide hormones and neuropeptides.<sup>27,28</sup> Because hydrogen bonding plays an essential role, the present system is also applicable to other types of biologically important guests. For example, peptide–nucleotide and peptide–sugar interactions can be conceived as major targets. Nucleotides such as NAD, FAD, and ATP are known as cofactors of enzymes and are tightly bound to apoproteins at recognition domains with  $\alpha/\beta$  structure.<sup>29</sup> Peptide structures that mimic these domains may be created on the surface of the monolayer. Model systems for the recognition of sugar by lectins<sup>30</sup> and ganglioside by hemagglutinin<sup>31–33</sup> may be designed. It is interesting to prepare amphiphiles that mimic a cell adhesion factor such as the RGD sequence.<sup>27,28</sup>

One of the most useful advantages in the current system is molecular variety. Diverse binding sites are created by mixing of relatively simple components. Molecular recognition by peptide monolayers may become a powerful tool of biomimetic chemistry.

LA981047P

(27) *Peptides: Chemistry and Biology*; Smith, J. A., Rivier, J. E., Eds.; ESCOM: Leiden, 1992.

(28) Alberts, B.; Bray, D.; Lewis, J.; Raff, M.; Roberts, K.; Watson, J. D. *Molecular Biology of the Cell*, 2nd ed.; Garland: New York, 1989.

(29) Branden, C.; Tooze, J. *Introduction to Protein Structure*; Garland: New York, 1991.

(30) Sharon, N.; Lis, H. *Lectins*; Chapman and Hall: New York, 1989.

(31) Wiley, D. C.; Wilson, I. A.; Skehel, J. J. *Nature* **1981**, *289*, 363.

(32) Suzuki, Y. *Prog. Lipid Res.* **1994**, *33*, 429.

(33) Sato, T.; Serizawa, T.; Okahata, Y. *Biochim. Biophys. Acta* **1996**, *1285*, 14.